Modelling the Effect of Turbulence Length Scale on Tidal Turbine Wakes using Advanced Turbulence Models

T. Ebdon[*‡], D.M O'Doherty [†], T. O'Doherty [*§], A. Mason-Jones [*¶]

[*]School of Engineering, Cardiff University, Cardiff, United Kingdom

[‡]EbdonT@cardiff.ac.uk

[§]odoherty@cardiff.ac.uk

[¶]Mason-JonesA@cardiff.ac.uk

[†]School of Engineering, University of South Wales, Pontypridd, United Kingdom

daphne.odoherty@southwales.ac.uk

Abstract—A numerical model using a hybrid turbulence model has been created for a 1/20th scale horizontal axis tidal stream turbine in a recirculating flume. In order to asses the suitability of the hybrid turbulence model for this application, the numerical model was validated against an experimental case, and the ability of the model to reproduce both the wake and performance of the turbine was evaluated. The hybrid model showed a greatly improved ability to predict wake recovery compared to a two-equation Reynolds Averaged Navier-Stokes (RANS) turbulence model, as well as improvements in the prediction of load fluctuations on the turbine. The hybrid model was then used to examine the effects of ambient turbulence length scale on the rate of wake recovery and indicates that the wake of a turbine is sensitive to turbulence length scale in a way not seen with the RANS model.

NOMENCLATURE

A	=	rotor swept area, m^2
C_{des}	=	DES calibration constant
C_P	=	power coefficient
C_T	=	thrust coefficient
C_θ	=	torque coefficient
D	=	rotor diameter, m
F_{DES}	=	DES turbulent kinetic energy dissipation multiplier
F_t	=	thrust force on turbine
k	=	turbulent kinetic energy
L_t	=	turbulent length scale
r	=	turbine radius, m
y_+	=	dimensionless wall coordinate
Δ_{max}	=	local maximum cell dimension
δ_{ij}	=	Kronecker delta
μ_t	=	turbulent viscosity
ρ	=	fluid density
τ	=	turbine torque
ω	=	turbine angular velocity
ω	=	specific dissipation rate
Y_k	=	turbulent kinetic energy dissipation term

I. INTRODUCTION

Studies of the potential of tidal stream energy resources have shown that relatively compact geographical regions are appropriate for energy generation with the current turbine technology. This geographical limitation arises not just due to the uneven distribution of energy density (i.e. regions of greater flow velocity), but also due to other factors important in the deployment of tidal turbines, such as the proximity of these areas to energy infrastructure on land, water depth, local bathymetry and seabed conditions[1]. Due to this, the areas appropriate for turbine deployment are expected to be populated with arrays of turbines, in order to extract the maximum amount of energy from the limited area.

Concentrating turbines together in close proximity to one another inevitably means that there will be interactions between them, which will have implications for the ultimate goal of energy extraction, as well as potentially for structural loading on the tidal turbines. These effects may be both positive and negative; whilst it is clear that there is less energy available in the decelerated flow downstream of a turbine, some studies have suggested that it may be possible to use local blockage effects around a turbine to increase energy extraction[2][3]. An understanding of, and the ability to predict these inter-turbine interactions will lead to the optimisation of array layouts, taking into account the potential for power extraction as well as the economic implications of increasing the loading on turbines.

In order to predict and characterise these inter-turbine interactions, it is important to be able to accurately model the wake created by a turbine; both its extent, as well as its nature. Ultimately, the ability to predict the combined wake of an array of tidal turbines is necessary to allow the modelling of the potential wider environmental impacts of tidal turbine

arrays, such as the sediment transport, which studies have shown could have potential impact on a regional scale[4], or an impact on flood risk and tidal times[5].

To date, many computational studies have been conducted into tidal turbines using Reynolds Averaged Navier-Stokes (RANS) turbulence models. Many of these have focussed on the the performance characteristics of the turbine, such as the power coefficient C_P, thrust coefficient C_T, or torque coefficient C_θ. It has been shown that these turbulence models are capable of producing a good match to turbine performance characteristics determined experimentally in low-turbulence flume, or zero-turbulence towing tank experiments. However, these models have been shown to be less accurate in their predictions of the length of turbine wakes[6], and their focus on time-averaged flow variables means that the data which they can provide about the character of the wake is limited.

The wake region behind a horizontal axis tidal turbine (HATT) is characterised by a region of highly turbulent flow of reduced velocity compared to the free stream. The length scales of turbulence expected in this region can be expected to be comparable to the width of the turbine, and flume tank experiments have shown that the turbulence in this region displays a high degree of anisotropy[7]. In addition to this, measurements at potential sites for tidal turbines have shown the flow to be highly turbulent and the size of the turbulent features present to be of the same order of magnitude as the diameter of a turbine[8]. RANS models which use the Boussinesq hypothesis rely on an assumption that turbulence is isotropic; an assumption which is reasonable for turbulence of a small length scale, but which is not appropriate for turbulence with a large length scale[9]. It is thought that this assumption within some RANS turbulence models may lead to their weakness when predicting wake length.

The aim of this study is to examine the use of a scaleresolving turbulence model (in this case, Detached Eddy Simulation (DES), which may be considered to be a hybrid RANS/Large Eddy Simulation (LES) model) for the modelling of turbine wakes, in order to see what improvements in accuracy this model potentially yields, as well as to examine any associated increases in computational costs. The CFD model will then be used to examine what effect ambient turbulence length scale may have on the rate of turbine wake recovery.

II. SIMULATION METHODOLOGY

Turbulence is a quasi-random phenomenon present in almost all engineering flows. It has a great effect on the characteristics of a flow and is particularly important for mixing, flow attachment and heat transport. In flows where turbulence is present, its presence must be accounted for in order to produce accurate simulations of the flow.

A common approach to modelling turbulence is through the use of the so-called Reynolds Averaged Navier-Stokes (RANS)

turbulence models. These are based on the principle of Reynolds decomposition to transform instantaneous flow variables such as velocity, u, or a scalar, φ, into a mean and a fluctuating component:

$$u = U + u^0 \qquad \varphi = \Phi + \varphi^0 \qquad (1)$$

These decomposed variables are substituted into the instantaneous non-compressible Navier-Stokes equations and timeaveraged, generating equations for the mean flow variables and

also giving rise to an extra term $\tau_{ij} = -\rho \overline{u^0_i u^0_j}$, known as the Reynolds stresses. This represents the transport of momentum between the mean and the fluctuating flow components, and must be modelled in order to allow closure of the NavierStokes equations.

Different models of varying complexity are available for the modelling of the Reynolds stresses. These range from simple, one-equations models such as the Spalart-Allmaras model, through two-equations models such as the k-ε, k-ω and k-ω SST models, through to the Reynolds Stress Model (RSM) which requires seven transport equations to be solved for closure in three dimensions. RANS models have been the mainstay of turbulence modelling for engineering flows for over thirty years, and as such the behaviour, strengths and weaknesses of each models are well known, with some models showing better performance than others for different categories of flows.

One of the disadvantages of the two-equation RANS models, is that they rely on the Boussineq hypothesis (equation 2) to relate the Reynolds stresses to the mean rates of deformation.

$$\tau_{ij} = -\rho \overline{u'_i u'_j} = \mu_t \left(\frac{\partial U_i}{\partial x_j} + \frac{\partial U_j}{\partial x_i} \right) - \frac{2}{3} \rho k \delta_{ij}$$

(2)

where $k = \frac{1}{2}(\overline{u'^2 + v'^2 + w'^2})$ is the turbulent kinetic energy, and δ_{ij} is the Kronecker delta. This equal division of kinetic energy over the three Cartesian directions implies isotropy of turbulence, and whilst this may a reasonable assumption for small scale turbulence, it is inappropriate for turbulence which has a large length scale[9]. In addition to this, measurements of the turbulence downstream of a prototype HATT have shown significant levels of anisotropy[7].

A different approach to accounting for the effects of turbulence is known as Large Eddy Simulation (LES). LES filters the Navier-Stokes equations in either physical or wavenumber space, with turbulent fluctuations larger than the filter width being directly resolved, and a sub-grid scale model being applied to fluctuations smaller than the filter width. The advantage of this approach is that the largest length scales

which are both the most anisotropic as well as contain the highest proportion of turbulent kinetic energy are directly resolved, with only the smaller length scale turbulence being treated as isotropic. In addition to this, because LES resolves the turbulent fluctuations themselves, rather than modelling the effect of turbulence on the mean flow, it allows the collection of statistics relating to the turbulent fluctuations in the flow.

The disadvantage of LES is the greatly increased computational expense when compared to two-equation RANS models. This stems from the increased mesh requirements of LES, as well as the need for more time steps in order to get statistically steady values for the flow statistics. In finite volume CFD, the cell dimensions are commonly used as the LES filter width (if filtering is carried out in physical space), which means that the cells require a lower aspect ratio when compared to those acceptable for RANS simulations. This has the effect of increasing the number of cells required in the stream-wise direction. Turbulence length scale decreases as the distance to boundary walls decreases, with the consequence that the largest eddies in this region (and thus the eddies containing the most turbulent kinetic energy) are much smaller than those in the free stream. In order to resolve these large eddies, the local cell size must also be reduced, leading to LES requiring a much higher cell density in the boundary layer region than RANS models. For LES, the recommended value of dimensionless wall coordinate, y^+ is $y^+ \approx 1$, whereas for the k-ω SST model the recommended maximum is $y^+ \approx 400$– 500[10][9]. This combination of low aspect ratio cells in the free stream and stringent y^+ requirements at boundaries means that meshes for LES necessarily have a much higher cell count than RANS models.

The current study models turbulence using Detached Eddy Simulation (DES), which can be thought of as a hybrid RANS/LES model, which attempts to combine the accuracy of the LES model in the highly detached region with the computational efficiency of a two-equation RANS model in the near-wall regions. The processes of time averaging (for RANS models) and spatial averaging (LES) may be combined once it is recognised that, once averaging has been carried out, all information pertaining to the process by which the averaging has taken place is lost. Both RANS and LES effectively become turbulence viscosity models, albeit applying a different method to calculate the local turbulent viscosity[10]. DES exploits this by using RANS methods for the calculation of the turbulence viscosity in near-wall regions, and LES-like methods far from walls. This reduces the near-wall mesh requirements otherwise needed for LES, therefore reducing computational cost. The DES model used here is based on the k-ω SST turbulence model, and switches to 'LES mode' by reducing the turbulence viscosity via a modification of the kinetic energy dissipation term, Y_k, in the transport equation for k. Where DES applies the pure RANS models and where it recovers LES-like behaviour is determined by a comparison of the maximum local cell dimension, Δ_{max} and the local turbulent length scale, L_t.

$$Y_k = \rho\beta^*k\omega \qquad \text{becomes} \quad Y_k = \rho\beta_*k\omega F_{DES} \qquad (3)$$

$$\text{where} \quad F_{DES} = max\left(\frac{L_t}{C_{des}\Delta_{max}}, 1\right) \qquad (4)$$

Here, L_t represents the turbulence length scale, defined by:

$$L_t = \frac{\sqrt{k}}{\beta_{*\omega}} \qquad (5)$$

Where ω here represents the specific dissipation rate. A complete definition of β_* can be found in [10], but is not included here for brevity.

When using the DES turbulence model, it is important that the user be aware of where the model is running in 'RANS mode' and where it is running in 'LES mode'. One way of determining which treatment the model is applying to a specific region is by analysing F_{DES}. By inspection of equation 3, it can be seen that when $F_{DES} = 1$, then Y_k is unchanged, and the model is operating as the unmodified k-ω SST model – i.e. in 'RANS mode'. Where $F_{DES} 6= 1$, then Y_k has been altered, and the model is running in 'LES mode'. In order to easily identify the areas in which 'RANS mode' and 'LES mode' have been applied, the value of $1/F_{DES}$ has been plotted on the horizontal plane containing the axis (figure 1). Where $1/F_{DES} < 1$, then the model can be considered to be in 'LES mode', and where $1/F_{DES} = 1$, then it can be considered to be running in 'LES mode'. Figure 1 shows that the RANS model is being applied to the flume walls and turbine surfaces, with turbulence being resolved in and around the wake region, as well as upstream of the turbine. This demonstrates that the model is working as desired.

Whilst DES has reduced mesh requirements and therefore reduced computational expense when compared to LES, it still requires significantly more computational resources than a pure RANS model. One of the reasons for this is that DES attempts to resolve turbulent flow features, whereas RANS models do not resolve the features themselves, but rather attempt to show the *effect* of these features on the mean flow. Mean flows are calculated in DES by sampling the instantaneous flow field over many time steps. In order to make the difference between the types of output from the models clear, figure 2 shows results for normalised streamwise velocity, obtained from the instantaneous DES flow field (top), time-averaged DES flow field (middle) and RANS flow field (bottom). The difference in the character of the velocity fields can be clearly seen. The resolution of the turbulent features in the instantaneous DES flow field means that characteristics such as RMS velocities can be obtained by directly sampling the instantaneous flow field (comparable to an experimental measurement with a LDA device), rather than from sampling of the already time-averaged velocities as in the RANS models.
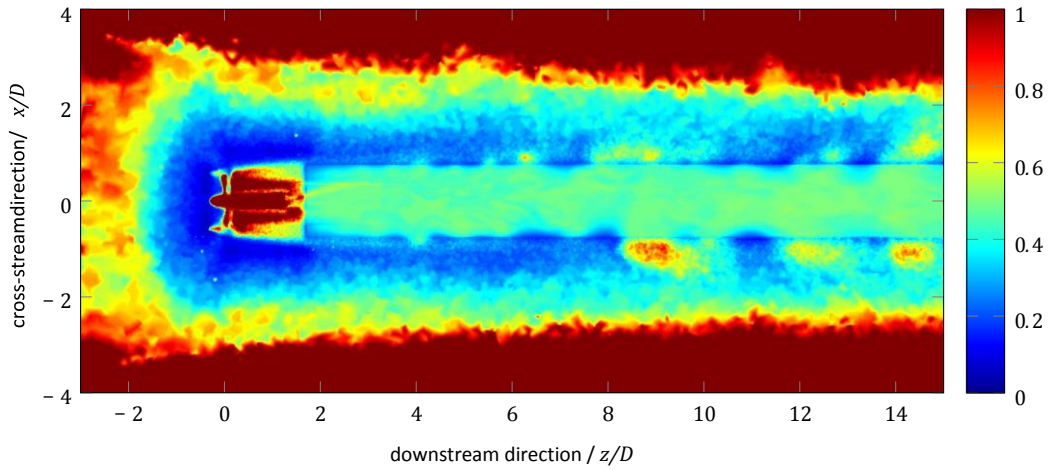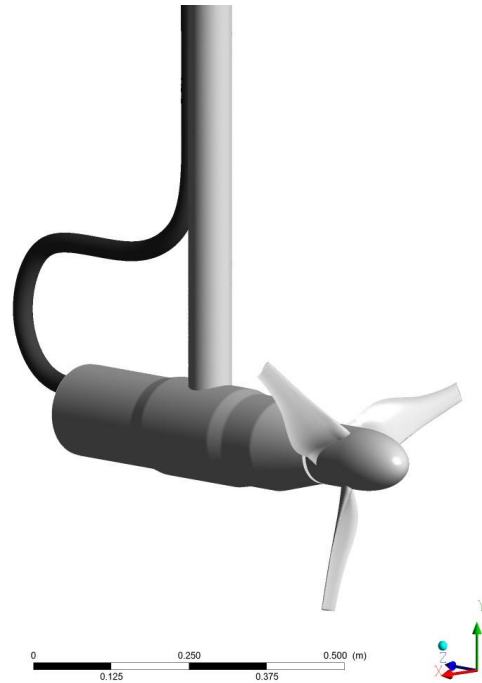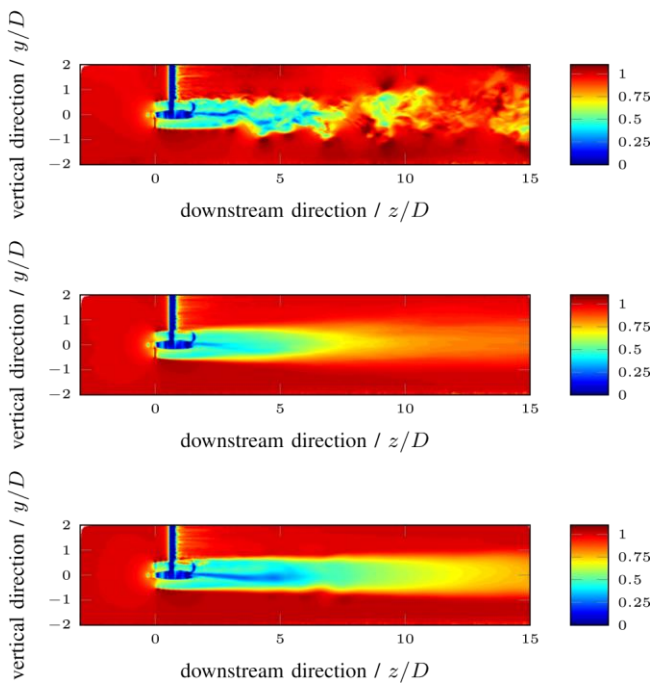
Fig. 1. $1/F_{DES}$, shown on the horizontal plane containing the turbine axis for the CFD validation case.

Fig. 2. Comparison of the different types of results yielded by the three models for the same boundary conditions. From top to bottom: instantaneous z-velocity from DES, time-averaged z-velocity from DES, mean z-velocity from RANS

However, the need for sampling over a large flow-time in order to obtain statistically steady results does increase the length of time required for these results to be obtained. Higher order statistics such as integral length scales require longer run times than lower order statistics such as mean velocity, in the same way as for flume tank experiments such as those detailed in [11].

III. MODEL GEOMETRY AND SETUP

A. Turbine and flume geometry

For this study, the recirculating flume of the Institut français de recherche pour l'exploitation de la mer (IFREMER) in Boulogne-sur-Mer was used. This flume has a capacity of approximately 700 m³ of water, with a working section 4 m wide, 2 m deep, with a maximum usable length of approximately 18 m.

The turbine used in the flume tank experiments was a 3bladed, 0.5 m rotor diameter design. The blade geometry is based on a Wortmann FX 63-137 section, with a twist of 30° from root to tip. Further details of the blade geometry can be found in [6] and [12]. The stainless steel turbine nacelle had a total length of 763 mm, and a maximum diameter of 160 mm. A hydraulic hose protruding from the downstream end of the turbine was used to house electrical cabling for motor power

and instrumentation. The whole turbine assembly was suspended in the centre of the cross-sectional area of the flume by a 71 mm diameter steel stanchion. The complete turbine geometry including rotor, nacelle, hose and stanchion was reproduced for the CFD model.

Fig. 3. The turbine modelled in this work

B. CFD model

A fluid domain was created in ANSYS Fluent® 15.0 in order to reproduce the experimental setup of the flume with a 0.5 m diameter turbine. The full width and depth of the flume was reproduced in the CFD domain, which extended from 1.5 m upstream of the plane of the turbine rotor to 7.5 m downstream of the plane of the turbine rotor. A noslip boundary condition was applied to the walls and bed of the flume, and a specified shear of zero was applied to the top boundary.

The fluid domain was divided into five regions in order to allow for turbine rotation and improve mesh control. The turbine rotor and spinner were incorporated into a cylindrical subdomain, coaxial to the turbine. This cylindrical subdomain was rotated at a rotational velocity of ω = 21.89 rad/s using a sliding mesh scheme. The sliding mesh scheme, in contrast to the multiple reference frame approach, allows the modelling of effects which arise from the asymmetry of the geometry, such as the interaction between passing turbine blades and the support stanchion.

Downstream of the turbine nacelle, a cylindrical region coaxial to the turbine but with a diameter of 0.75 m was created and meshed using a structured, swept mesh. The addition of this region allowed greater control over the mesh characteristics, allowing the density to be increased in the wake region itself as well as in the shear region between the wake and the free stream.

The turbine nacelle, stanchion and hose were meshed in a separate region of unstructured mesh in order to ease the meshing of this region of complex geometry. The rest of the fluid domain was divided into two regions using a plane normal to the stream-wise direction, at the downstream face of the rotating cylinder containing the turbine rotor. This separation of the region of the flume upstream of the turbine from that downstream of the turbine allowed for more mesh control of the upstream region, in order to ensure that turbulent features entering the domain through the inlet could be properly resolved.

Selection of mesh densities in all regions was based on previous studies of this turbine and its wake, and have been shown to be fine enough that the wake length and character is independent of the mesh. Mesh densities in the rotating mesh region surrounding the turbine rotor have been shown by previous studies to be sufficient for a mesh-independent solution [13], [12], and values of $y^+ \approx 40$ were achieved on the outboard regions of the suction side of the blades–well within the recommended values for the k-ω SST model used in this region.

The aim of this study is to examine the effects of ambient turbulence length scale on the wake of a tidal stream turbine. In order to isolate length scale from other turbulence effects which have been shown to affect the wake such as turbulence intensity[14][15], CFD runs for two different ambient turbulence length scales have been carried out. For validation of the CFD results, comparison is made for one case to experimental measurements conducted in a large recirculating flume tank.

IV. EXPERIMENTAL SETUP

For comparison with and validation of the CFD model, experimental measurements were carried out in the recirculating flume tank described in section III. Wake measurements were conducted on a horizontal plane downstream of the turbine, at distances of $4 \leq z/D \leq 15$ downstream of the plane of the rotor. In the cross-stream direction, measurements were made at $-1.6 \leq x/D \leq +1.6$ about the axis of the turbine. All measurements were made using a DANTEC Laser Doppler Anemometer (LDA), with an average sample rate of approximately 160 Hz, and sample times of 100 s, which have been shown to be sufficiently long to allow reliable calculation of statistical information about the flow (mean velocities, turbulence intensity etc.)[11]. In addition to this, measurements were made at a distance of z/D = 3 upstream of the turbine plane to characterise the flow profile of the tank, as well as the inflow conditions experienced by the turbine. For all the flow measurements detailed in this work, calculations of 1-dimensional turbulence intensity were made using equation 6, and integral length scale calculated by multiplying the integral time scale I obtained from equation 7 by the average velocity, U.

$$TI = 100 \times \frac{\sqrt{\overline{u'^2}}}{U} \tag{6}$$

$$I = \int_0^\infty \rho(s)\mathrm{d}s \quad \text{where:} \quad \rho(s) = \frac{\overline{u'(t)u'(t+s)}}{\overline{u'^2}} \tag{7}$$

Using these formulae, the ambient flow conditions for the wake measurements were U = 1.5 m/s, TI = 1.75% and turbulence length scale, l = 0.5 m. In addition to wake measurements, the turbine is instrumented to allow measurements of turbine torque (via the torque-generating current), and rotational velocity, both sampled at 16.6 Hz. The stanchion from which the turbine was suspended was instrumented with four strain gauges in a full-bridge configuration, in order to measure the thrust on the turbine. These measurements were used with equations 8 to 10 to

calculate the turbine power coefficient, C_P, thrust coefficient, C_T and torque coefficient, C_θ.

$$C_P = \frac{\tau\omega}{0.5\rho Av^3} \tag{8}$$

$$C_T = \frac{F_T}{0.5\rho Av^2} \tag{9}$$

$$C_\theta = \frac{\tau}{0.5\rho Av^2 r} \tag{10}$$

These performance characteristics are also important in the assessment of the accuracy of a CFD model, and although they are not the main focus of this work, they are nonetheless included for comparison.

V. RESULTS

The results section is split in to two parts. The first deals with the validation of the CFD model by comparison with the flume test case, in order to give confidence in the suitability of DES for this particular application. The second part compares two different CFD simulations, which model an identical geometry, differing only in the length scale of the turbulence at the upstream boundary.
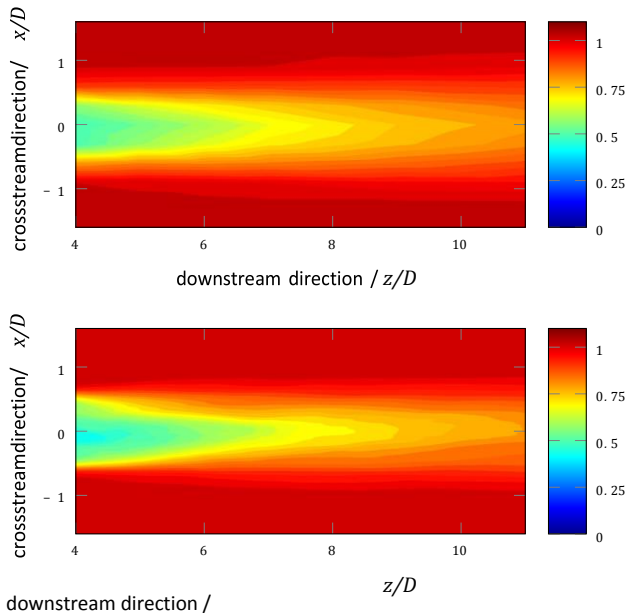

Fig. 4. Comparison of normalised mean stream-wise velocity between CFD and experimental measurements. Top is experimental results, bottom is CFD results.

A. CFD validation

To provide confidence in the ability of the DES turbulence model to reproduce the wake behind a tidal stream turbine, it

has been compared to a flume tank experiment using identical geometry and flow conditions. For visual comparison, the time averaged stream-wise velocity measured in a region from $4D$ to $11D$ downstream is compared in figure 4. Inspection of these two velocity maps show good agreement in the overall rate of wake recovery and the shape of the wake. Indeed, even the slight asymmetry in the wake apparent in the experimental results is reproduced in the computational model. It is hypothesised that the asymmetry is the result of the rotational asymmetries in the geometry of the flume setup (presence of the stanchion and differences in boundaries due to the presence of a free surface). It should be noted that the experimental wake does appear to be slightly wider than the CFD wake (figure 4).

A clearer idea of the level of agreement between the CFD and experimental results can be gained from figures 5 and 6, which shows the ability of the CFD to replicate the results at the specific points at which the wake measurements were made. Figure 5 compares measurements of stream-wise velocity downstream of the turbine to those obtained from the CFD results using both the DES and RANS (k-ω SST) turbulence models. Good agreement between experimental and DES is shown for the centreline velocity measurements with an apparent tendency for the CFD to slightly under predict the level of wake recovery in the near wake ($z/D < 8$). An alternative metric for a designer wishing to optimise turbine layout in an array is the volumetric flow rate across the swept area of the turbine. This gives an indication of the
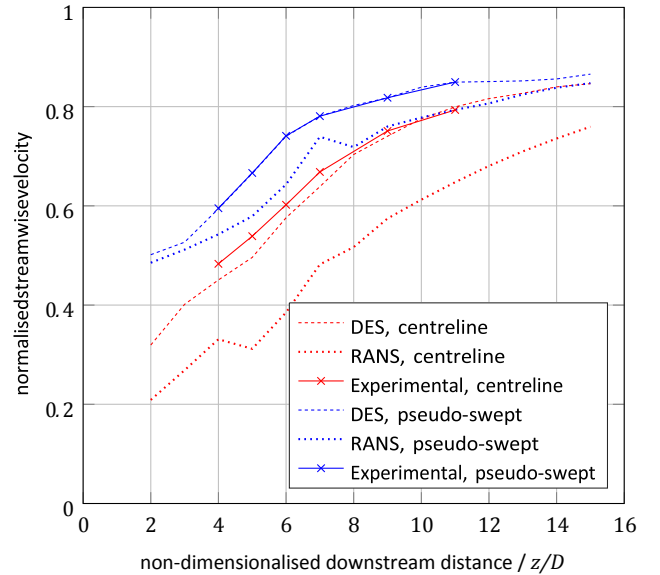

Fig. 5. Comparison of CFD and experimental plots. Crosses mark the downstream positions at which experimental measurements were made.

maximum amount of energy available in the flow for a turbine to extract. Whilst it is relatively straightforward to obtain the mean volumetric flow rate across the entire swept area of the

turbine in CFD post processing, the experimental wake measurements have only been made in the horizontal plane. To produce a volumetric flow rate across the turbine area from the experimental results, a shell integration was carried out on the velocity profile rakes. In order to account for crossstream wake asymmetry, this procedure was carried out for each side of the profile, and the average taken, similar to the method used in [14]. A direct comparison of the integrated velocities from the experimental rake and the complete swept area from CFD would be inappropriate, due to the influence of the stanchion in the upper part of the wake. Therefore, point values of mean velocity have been extracted from the CFD at the same positions as the experimental measurements were made, and the same integration procedure carried out on these. The resulting curves are shown in figure 5, with the DES turbulence model showing excellent agreement across the full range of the experimental data. Both centreline and pseudo-swept velocities predicted by the RANS model are also included in figure 5. These results show that the RANS model strongly under predicts the rate of wake recovery, with the largest discrepancies apparent for the centreline measurement.

Comparisons of rakes through the wake region for DES and the experimentally measured wake are presented in figure 6. Mean stream-wise velocity data has been extracted at identical points in the flow field and the results plotted for six downstream stations. These confirm the qualitative observations made from figure 4, that the CFD results also demonstrate a slight asymmetry, and the quantitative observations of figure 5, that the CFD model slightly under predicts the rate of centreline wake recovery. The reason for the excellent match
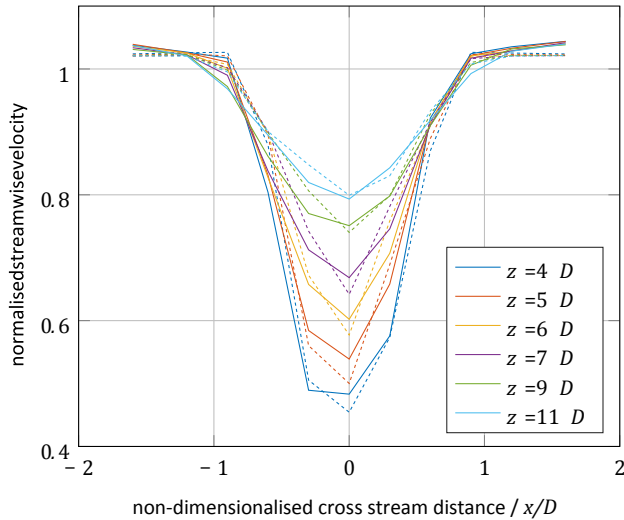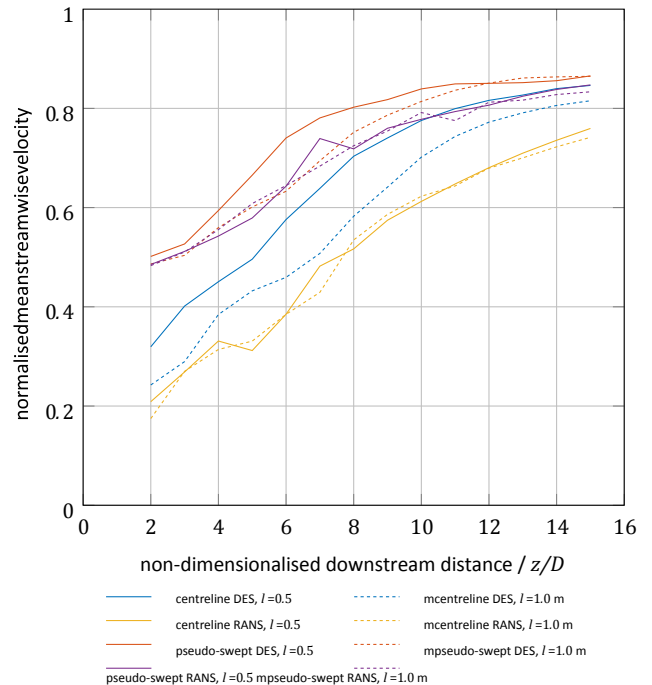
TABLE I
TURBINE PERFORMANCE DATA, COMPARISON BETWEEN CFD AND EXPERIMENTAL

		Experiment	DES	RANS
C_P	mean	0.391	0.441	0.443
	σ	0.0201	0.0089	0.00011
C_T	mean	1.056	0.864	0.870
	σ	0.0244	0.0103	0.0003
C_θ	mean	0.107	0.121	0.121
	σ	0.0055	0.0024	0.00003

of volumetric stream-wise velocity over the swept area also becomes clear – despite the slight differences in shape, the area under pairs of curves in figure 6, as well as the radial distribution of area is almost identical.

Whilst not the main focus of this study, turbine performance data, (C_P, C_T, C_θ) have also been measured in both the experimental and CFD cases. These are compared in table I. From this table, it can be seen that the CFD over predicts C_P and C_θ, whilst under predicting C_T. It should be noted however, that previous flume tank measurements with this turbine blade geometry suggest a slightly higher C_P [6][13]. In all cases, the standard deviations are under-predicted by the CFD, although, as this is a higher-order statistic, these are expected to be less reliable than the values for the means. A comparison of the turbine performance characteristics obtained from RANS and DES turbulence models show only very slight differences in the mean values for each of C_P, C_T and C_θ. However, the standard deviations differ between the RANS and DES models by approximately two orders of magnitude, with the standard deviations obtained from the DES model being a much better approximation of those obtained experimentally than those obtained from the RANS model.

Fig. 6. Comparison of CFD and experimental data for downstream stations. Dashed lines indicate CFD data.

Fig. 7. Wake recovery curves for CFD simulations, length scales l =0.5 m and l =1.0 m.

B. Effect of turbulence length scale

Normalised wake recovery curves for input turbulence length scales of 0.5 m and 1.0 m are presented in figure 7. Recovery curves are shown for both mean centreline velocities as well as volumetric average velocities for the pseudo-swept area procedure described above. Results from both RANS and DES runs are included. The DES results show that both the centreline and pseudo-swept velocity recovers more quickly for the $l = 0.5$ m case than the $l = 1.0$ m case. For the pseudo-swept area curves, the difference in velocity recovery for the two cases becomes negligible beyond approximately z/D = 12. Given that there is still a difference in recovery for the centreline measurements, this suggests that the outer part of the wake has recovered more at these downstream distances in the $l = 0.5$ m case than the $l = 1.0$ m case.

Also included in figure 7 are wake recovery curves obtained from the RANS turbulent model. These show that not only does the RANS turbulence model significantly under-predict the rate of wake recovery, but also that the predicted rate of wake recovery from the RANS models appears independent of input turbulence length scale.

VI. DISCUSSION

A. CFD validation

The comparison of the CFD results using DES and the wake measured experimentally shows very good agreement for mean centreline velocities and excellent agreement when averaged over the swept-area of the turbine. These results show a significant improvement in accuracy over the $k\text{-}\omega$ SST RANS model.

TABLE II

TURBINE PERFORMANCE DATA, COMPARISON OF DIFFERENT TURBULENT LENGTH SCALES, l.

		$l = 0.5$ m		$l = 1$ m	
		RANS	DES	RANS	DES
C_P	mean	0.443	0.441	0.443	0.441
	σ	0.00011	0.0089	0.00012	0.0026
C_T	mean	0.870	0.864	0.870	0.863
	σ	0.00030	0.0103	0.00030	0.0034
C_θ	mean	0.121	0.121	0.121	0.121
	σ	0.00003	0.0024	0.00003	0.0007

This is thought to be due to DES more accurately modelling the complex mixing processes between the free stream and wake regions, which is a major determining factor in the rate of wake recovery. However, DES requires significantly longer to run than RANS models in order to give confidence in the mean results, which are obtained via sampling the fluctuating instantaneous flow-field. Analysis of changes in the mean results with increasing sample time showed the sample time

used here to be sufficient for confidence in the mean velocities. Higher order statistical quantities such as RMS values of fluctuating velocities require larger sample times to reach stable values.

Agreement of CFD with experiment for turbine performance characteristics is less favourable, and agreement for C_T can be said to be poor. Mean values of C_P and C_θ were both over-predicted in CFD by approximately 13%, and mean C_T was under-predicted by approximately 22%. The CFD values presented here for C_P, C_T and C_θ are similar to previous reported values for this turbine blade geometry with a $k\text{-}\omega$ SST turbulence model [13]. The experimental values for C_P obtained in this experiment were lower than that measured in previous experiments with this blade geometry, which gave blockage corrected results of approximately C_P = 0.41, which would improve agreement with CFD results in this study[6][13]. There is little or no difference in the mean values of C_P, C_T and C_θ predicted by the DES and RANS turbulence models, however, the standard deviation of the RANS results is approximately two orders of magnitude lower than that of the DES results, which themselves are approximately half the size of the standard deviations of the experimental results. This indicates that the DES model may be more accurately representing the large-scale ambient turbulence and in turn, the fluctuations in turbine performance induced by this turbulence. If this is the case, then DES could prove to be a valuable tool for predicting the fluctuating forces experienced by a turbine in realistic ocean flows – something of great importance for the design of turbine structures.

B. Effect of turbulence length scale

Comparison of the CFD results for different length scales indicates that the larger length scale reduces the rate of wake recovery. This result indicates less mixing between the higherenergy free stream and the lower-energy wake regions. Whilst it might be expected that a larger turbulence length scale might improve momentum transfer between the wake and free stream, these results can perhaps be explained by considering the turbulence length scales as a proportion of the turbine size. When considered thus, the $l = 0.5$ m case can be considered $l = D$, and the $l = 1.0$ m case represents turbulence of a scale $l = 2D$. It is conceivable that when the turbulent length scale is significantly larger than the diameter of the turbine, the turbulent fluctuations no longer appear to the turbine as fluctuating velocity gradients across the face of the turbine, but rather as 'surges'; increasing the velocity over the swept area of the turbine in a more or less uniform manner. Large fluctuations such as this may therefore not increase the mixing of the high-energy free stream and low-energy wake regions when compared to turbulence of a length scale $l \approx D$, leading to a slower rate of wake recovery. The relationship between different turbulence length scales have and the rate

of wake recovery is expected to be complex, and is the subject of ongoing research.

VII. Conclusions and prospects

The DES model used in this work shows excellent agreement with the experimental case for mean velocities in the wake of a horizontal axis turbine. There is less agreement between the CFD and experimental case for the turbine performance characteristics, although the values of C_P, C_T and C_θ measured in previous flume experiments with this turbine blade geometry provide closer matches. This increase in accuracy for wake prediction of DES over a k-ω SST RANS model appears to have no negative effects on the prediction of mean turbine performance indicators, C_P, C_T and C_θ. Indeed, DES produces estimates for the fluctuations in these quantities which show much better agreement with the flume tank data than the estimates produced by the RANS model. However, whilst providing significant improvements in accuracy, DES requires longer run times than RANS in order to gain confidence in statistical quantities such as RMS velocity fluctuations. If it can be shown that DES also produces better estimates of the character of the wake, then it could prove an important tool for the designers of turbine structures.

Turbulence length scale appears to have a significant effect on the rate of wake recovery, and the way in which this influence manifests itself is expected to be complex. Further work, both numerical and experimental is required to fully understand the effect that turbulence length scale has on the wake.

The comparison of the test case with identical flow conditions is promising, and if DES is shown to be accurate in its predictions of turbine wakes for a wide variety of flow conditions, then it could prove to be a valuable tool for array layout optimisation. It could allow more accurate estimates to be made of the length and character of the wake of a tidal stream turbine, with important implications for the economics of turbine arrays from the point of view of both energyextraction and structural loading. DES could have the potential to provide accurate wake predictions for arrays of turbines, allowing estimates to be made of the far-field environmental effects of these turbines.

References

[1] AbuBakr S. Bahaj. Generating electricity from the oceans. *Renewable and Sustainable Energy Reviews*, 15(7):3399 – 3416, 2011.

[2] Ross Vennell, Simon W. Funke, Scott Draper, Craig Stevens, and Tim Divett. Designing large arrays of tidal turbines: A synthesis and review. *Renewable and Sustainable Energy Reviews*, 41:454–472, 2015.

[3] J. Schluntz and R.H.J. Willden. The effect of blockage on tidal turbine rotor design and performance. *Renewable Energy*, 81:432–441, 2015.

[4] Jer´ome Thiˆebot, Pascal Bailly du Bois, and Sylvain Guillou. Numerical´ modeling of the effect of tidal stream turbines on the hydrodynamics and the sediment transport – Application to the Alderney Race (Raz Blanchard), France. *Renewable Energy*, 75:356–365, 2015.

[5] D. Fallon, M. Hartnett, A. Olbert, and S. Nash. The effects of array configuration on the hydro-environmental impacts of tidal turbines. *Renewable Energy*, 64:10–25, 2014.

[6] A. Mason-Jones. *Performance assessment of a Horizontal Axis Tidal Turbine in a high velocity shear environment*. PhD thesis, School of Engineering, Cardiff University, 2010.

[7] S.C. Tedds, I. Owen, and R.J. Poole. Near-wake characteristics of a model horizontal axis tidal stream turbine. *Renewable Energy*, 63:222–235, 2014.

[8] I.A. Milne, R.N. Sharma, R.G.J. Flay, and S. Bickerton. Characteristics of the turbulence in the flow at a tidal stream power site. *Phil Trans R Soc A*, 371:20120196, 2013.

[9] H.K. Versteeg and W. Malalasekera. *An Introduction to Computational Fluid Dynamics, The Finite Volume Method*. Pearson Education Limited, 2007.

[10] ANSYS. *ANSYS Fluent Theory Guide*, November 2013. Release 15.0.

[11] Tom Blackmore, Luke E. Myers, and AbuBakr S. Bahaj. Effects of turbulence on tidal turbines: Implications to performance, blade loads, and condition monitoring. *International Journal of Marine Energy*, 14:1–26, 2016.

[12] A. Mason-Jones, D.M. O'Doherty, C.E. Morris, T. O'Doherty, C.B. Byrne, P.W. Prickett, R.I. Grosvenor, I. Owen, S. Tedds, and R.J. Poole. Non-dimensional scaling of tidal stream turbines. *Energy*, 44:820–829, 2012.

[13] Ceri Morris. *Influence of Solidity on the Performance, Swirl Characteristics, Wake Recovery and Blade Deflection of a Horizontal Axis Tidal Turbine*. PhD thesis, School of Engineering, Cardiff University, 2014.

[14] Paul Mycek, Benoˆıt Gaurier, Gregory Germain, Gr´egory Pinon, and´ Elie Rivoalen. Experimental study of the turbulence intensity effects on marine current turbines behaviour. part I: One single turbine. *Renewable Energy*, 66:729–746, 2014.

[15] Tom Blackmore, Benoˆıt Gaurier, Luke Myers, Gregory Germain, and AbuBakr S Bahaj. The Effect of Freestream Turbulence on Tidal Turbines. In *Proceedings of the 11th European Wave and Tidal Energy Conference, Nantes, France*, 6–11th Sept 2015.